

Experiment-based identification of time delays in linear systems

Meng-Shi Jin¹ · Yi-Qiang Sun² · Han-Wen Song¹ · Jian Xu¹

Received: 31 October 2016 / Revised: 9 December 2016 / Accepted: 22 December 2016 / Published online: 14 March 2017

© The Chinese Society of Theoretical and Applied Mechanics; Institute of Mechanics, Chinese Academy of Sciences and Springer-Verlag Berlin Heidelberg 2017

Abstract This paper presents an identification approach to time delays in single-degree-of-freedom (SDOF) and multiple-degree-of-freedom (MDOF) systems. In an SDOF system, the impedance function of the delayed system is expressed by the system parameters, the feedback gain, and the time delay. The time delay can be treated as the “frequency” of the difference between the impedance function of the delayed system and that of the corresponding uncontrolled system. Thus, it can be identified from the Fourier transform of the difference between the two impedance functions. In an MDOF system, the pseudo-impedance functions are defined. The relationships between the time delay and the pseudo-impedance functions of the delayed system and uncontrolled system are deduced. Similarly, the time delay can be identified from the Fourier transform of the difference between the two pseudo-impedance functions. The results of numerical examples and experimental tests show that the identification approach to keeps a relatively high accuracy.

Keywords Time-delay identification · Impedance function · Feedback controlled system

1 Introduction

In practical engineering, time delays exist in the process of active control, which has attracted the attention of researchers [1–3]. Researchers once ignored time delays as a simplification. However, it has been shown that ignoring time delays may lead to wrong conclusions [4]. Therefore, an approach to identifying time delays is necessary. This paper proposes such an identification approach to time-delay feedback. In a single-degree-of-freedom (SDOF) system, the impedance function is the reciprocal of the frequency response function (FRF). The impedance function of a delayed system is expressed by the system parameters, the feedback gain, and the time delay. The time delay can be identified from the difference between the impedance function of the delayed system and that of the corresponding uncontrolled system since the time delay acts as the “frequency” of the difference curve. Then we consider a multiple-degree-of-freedom (MDOF) system where the FRF matrix cannot be completely measured in an experiment. This means the inverse matrix of the FRF matrix, namely, the impedance function matrix, cannot be obtained. Therefore, a pseudo-impedance function is defined and applied to identify the time delay. Numerical simulations are presented to show the details of how time delays are identified in SDOF and MDOF systems. An experiment is conducted in an MDOF system with acceleration time-delay feedback. The identification results of the time delay demonstrate the high accuracy of the proposed identification approach.

In early papers, time delays were treated as negative because they could cause stable systems to become unstable [5,6]. However, a time delay does not always produce negative effects. Instead, the appropriate use of a time delay can help to improve the performance of a system [7–12].

✉ Han-Wen Song
hwsong@tongji.edu.cn

¹ School of Aerospace Engineering and Applied Mechanics, Tongji University, Shanghai 200092, China

² Shanghai Engineering Center for Microsatellites, Shanghai 201210, China

Whether a time delay brings harm or benefit to a system, it inevitably exists in many practical engineering cases, such as controlled wheel suspension systems and metal cutting chatter [13, 14].

Some evidence has shown that ignorance of time delays may cause people to mistakenly regard an unstable system with a time delay as stable or treat a stable system as unstable if they ignore the time delay of the original system [4].

Research results indicate that time delays cannot be ignored, so there must be some way to identify time delays [15–19]. Orlov et al. [15] developed a synthesis of an adaptive parameter identifier for linear systems with finitely many lumped delays in the state vector and control input. Once the state of the system and the parameter identifiability were guaranteed, online identification of the delays were achieved. Hidayat and Medvedev [16] proposed a method for Laguerre domain identification of continuous-time-delay systems from impulse response data. Gu et al. [17] proposed a general method to identify the time delays in delayed systems based on the autosynchronization technique. Na et al. [18] proposed a method of adaptive online parameter identification for linear single-input–single-output (SISO) time-delay systems that made it possible to estimate an unknown time delay. Karoui et al. [19] proposed a fast online identification algorithm for linear-time invariant multiple-time-delay systems. The identification problem of multiple-input–single-output systems with two unknown time delays was considered.

Although methods have been proposed to identify time delays in linear systems, little theoretical work besides that of Hu [20] has been published. In that paper [20], a time delay was identified in an SDOF system with different displacement and velocity time delay feedback. It was pointed out that if the system is subject to a harmonic input of frequency ω , the identified time delay may deviate from the real values by $2p\pi/\omega$, where p is a positive integer.

In the current paper, the basic idea of the identification approach comes from the difference between the impedance function of the delayed system and that of the corresponding uncontrolled system. Specifically, the difference is an oscillation curve in the frequency domain, with the time delay being its “frequency.” In the SDOF system, the time delay can be identified from the difference between the impedance function of the delayed system and that of the corresponding uncontrolled system. In the MDOF system, the pseudo-impedance function is defined in such a way as to play the same role as the impedance function in SDOF system. Furthermore, apart from numerical simulations in SDOF and MDOF systems, an experiment is conducted in an MDOF system with acceleration time-delay feedback. The identification results of the time delay demonstrate the high level of accuracy of the proposed approach.

The proposed identification approach has two features: (1) a time delay can be identified without being given an initial value in advance and (2) the approach is based on the data in the frequency domain instead of the time domain.

This paper is organized as follows. Theories of the identification approach to time delays in SDOF and MDOF systems are presented in Sect. 2. Numerical examples are provided in Sect. 3 to demonstrate the process of the identification. Section 4 shows an experiment where a time delay is identified in an MDOF system with acceleration time-delay feedback. Conclusions are provided in Sect. 5.

2 Identification approach

In this section, the measuring points of a system are divided into three types for the convenience of discussion. They are input points, reference points, and feedback points. An input point is a point upon which external force is applied. A reference point is a point whose controlling signal is collected before the feedback. A feedback point is a point where the feedback is applied.

2.1 SDOF system

The equation of motion in an uncontrolled linear system can be expressed as

$$m\ddot{x}(t) + c\dot{x}(t) + kx(t) = f(t), \quad (1)$$

where m , c , k , $f(t)$, $x(t)$ denote the mass, damping, stiffness, input, and displacement response, respectively.

We take the Fourier transform of Eq. (1) to obtain the equation of motion in the frequency domain [21]:

$$-\omega^2 mX(\omega) + j\omega cX(\omega) + kX(\omega) = F(\omega), \quad (2)$$

where ω denotes the frequency.

The acceleration impedance function $Z(\omega)$ and acceleration FRF $H(\omega)$ of the uncontrolled system are as follows

$$Z(\omega) = \frac{1}{(j\omega)^2} \frac{F(\omega)}{X(\omega)} = \frac{k - \omega^2 m + j\omega c}{(j\omega)^2}, \quad (3)$$

$$H(\omega) = \frac{1}{Z(\omega)} = \frac{(j\omega)^2}{k - \omega^2 m + j\omega c}. \quad (4)$$

The real part and imaginary part of $Z(\omega)$, denoted by $\text{Re}(Z(\omega))$ and $\text{Im}(Z(\omega))$ respectively, can be obtained as follows

$$\begin{aligned} \text{Re}(Z(\omega)) &= \frac{k - \omega^2 m}{-\omega^2}, \\ \text{Im}(Z(\omega)) &= \frac{c}{-\omega}. \end{aligned} \quad (5)$$

Since it is easy to measure the acceleration signal of a system, acceleration feedback is applied to the uncontrolled system. Thus, the equation of motion in a feedback controlled system can be written as

$$m\ddot{x}(t) + c\dot{x}(t) + kx(t) = f(t) + g\ddot{x}(t - \tau), \tag{6}$$

where $g\ddot{x}(t - \tau)$ refers to acceleration feedback, with τ being the time delay and g the feedback gain.

Like the process in the uncontrolled system (1), the acceleration impedance function $Z^D(\omega)$, and acceleration FRF $H^D(\omega)$ of the delayed system (6) are expressed as follows, with the superscript D denoting “delay”

$$Z^D(\omega) = \frac{k - \omega^2 m + j\omega c + \omega^2 g e^{-j\tau\omega}}{(j\omega)^2}, \tag{7}$$

$$H^D(\omega) = \frac{1}{Z^D(\omega)} = \frac{(j\omega)^2}{k - \omega^2 m + j\omega c + \omega^2 g e^{-j\tau\omega}}. \tag{8}$$

The real and imaginary parts of $Z^D(\omega)$, denoted by $\text{Re}(Z^D(\omega))$ and $\text{Im}(Z^D(\omega))$ respectively, are expressed as follows

$$\begin{aligned} \text{Re}(Z^D(\omega)) &= \frac{k - \omega^2 m}{-\omega^2} - g \cos(\tau\omega), \\ \text{Im}(Z^D(\omega)) &= \frac{c}{-\omega} + g \sin(\tau\omega). \end{aligned} \tag{9}$$

Subtracting Eq. (5) from Eq. (9), we obtain

$$\begin{aligned} \text{Re}(Z^D(\omega)) - \text{Re}(Z(\omega)) &= -g \cos(\tau\omega), \\ \text{Im}(Z^D(\omega)) - \text{Im}(Z(\omega)) &= g \sin(\tau\omega). \end{aligned} \tag{10}$$

It can be seen that the difference between $\text{Re}(Z(\omega))$ and $\text{Re}(Z^D(\omega))$ is a harmonic function, with time delay τ being the “frequency.” The difference between the two imaginary parts has the same feature.

Therefore, τ can be identified from the difference between the real parts of the two acceleration impedance functions of the uncontrolled and delayed systems. Similarly, τ can also be identified from the difference between the imaginary parts of the two acceleration impedance functions. It should be noted that τ is identified from a frequency domain curve since ω is the independent variable.

2.2 MDOF system

The equation of motion in an uncontrolled linear system with n degrees of freedom (DOF) can be given as

$$M\ddot{X}(t) + C\dot{X}(t) + KX(t) = F(t), \tag{11}$$

where $M, C, K, F(t), X(t)$ denote the mass matrix, damping matrix, stiffness matrix, input, and displacement response, respectively. M is a diagonal matrix, and C and K are positive definite real symmetric matrices.

We now take the Fourier transform of Eq. (11) to obtain the equation of motion in the frequency domain:

$$-\omega^2 MX(\omega) + j\omega CX(\omega) + KX(\omega) = F(\omega). \tag{12}$$

The acceleration impedance function matrix $Z(\omega)$ of the uncontrolled system is expressed as follows

$$Z(\omega) = \frac{1}{(j\omega)^2} \frac{F(\omega)}{X(\omega)} = \frac{(K - \omega^2 M + j\omega C)}{(j\omega)^2}. \tag{13}$$

The acceleration FRF matrix is the inverse matrix of the acceleration impedance function matrix:

$$\begin{aligned} H(\omega) = Z^{-1}(\omega) &= \frac{\text{adj}(Z(\omega))}{\det(Z(\omega))} \\ &= \frac{1}{\det(Z(\omega))} \begin{bmatrix} A_{11}(\omega) & A_{21}(\omega) & \cdots & A_{n1}(\omega) \\ A_{12}(\omega) & A_{22}(\omega) & \cdots & A_{n2}(\omega) \\ \vdots & \vdots & \ddots & \vdots \\ A_{1n}(\omega) & A_{2n}(\omega) & \cdots & A_{nn}(\omega) \end{bmatrix}, \end{aligned} \tag{14}$$

where $\det(Z(\omega))$ is the determinant of $Z(\omega)$. $\det(Z(\omega))$ is a polynomial function of ω , denoted by $\Phi(\omega)$. $A_{pq}(\omega)$, the algebraic cofactor of $Z(\omega)$, is also a polynomial function of ω . Any element $H_{pq}(\omega)$ of $H(\omega)$ can be expressed as

$$H_{pq}(\omega) = \frac{A_{qp}(\omega)}{\det(Z(\omega))} = \frac{A_{qp}(\omega)}{\Phi(\omega)}, \quad p, q = 1, 2, \dots, n. \tag{15}$$

In the case of acceleration time-delay feedback, the equation of motion can be given as

$$M\ddot{X}(t) + C\dot{X}(t) + KX(t) = F(t) + G\ddot{X}(t - \tau), \tag{16}$$

where $G\ddot{X}(t - \tau)$ refers to the acceleration feedback matrix, with τ being a time delay and G being the feedback gain matrix.

We now take the Fourier transform of Eq. (16) to obtain the equation of motion in the frequency domain:

$$\begin{aligned} -\omega^2 MX(\omega) + j\omega CX(\omega) + KX(\omega) \\ = F(\omega) - \omega^2 G e^{-j\omega\tau} X(\omega). \end{aligned} \tag{17}$$

The acceleration impedance function matrix $\mathbf{Z}^D(\omega, \tau)$ of the delayed system can be expressed as follows

$$\mathbf{Z}^D(\omega, \tau) = \frac{(\mathbf{K} - \omega^2 \mathbf{M} + j\omega \mathbf{C} + \omega^2 \mathbf{G}e^{-j\omega\tau})}{(j\omega)^2}. \tag{18}$$

Set point r as the reference point and all the measuring points as the feedback points. The feedback gain matrix \mathbf{G} has only one column of nonzero elements:

$$\mathbf{G} = \begin{bmatrix} 0 & \cdots & g_{1r} & \cdots & 0 \\ \vdots & \ddots & \vdots & \ddots & \vdots \\ 0 & \cdots & g_{rr} & \cdots & 0 \\ \vdots & \vdots & \vdots & \ddots & \vdots \\ 0 & \cdots & g_{nr} & \cdots & 0 \end{bmatrix}. \tag{19}$$

Then $\mathbf{Z}^D(\omega, \tau)$ can be expressed in detail as

$$\mathbf{Z}^D(\omega, \tau) = \frac{1}{(j\omega)^2} \begin{bmatrix} k_{11} - \omega^2 m_1 + j\omega c_{11} & k_{12} + j\omega c_{12} & \cdots & k_{1r} + j\omega c_{1r} + \omega^2 g_{1r} e^{-j\omega\tau} & \cdots & k_{1n} + j\omega c_{1n} \\ k_{21} + j\omega c_{21} & k_{22} - \omega^2 m_2 + j\omega c_{22} & \cdots & k_{2r} + j\omega c_{2r} + \omega^2 g_{2r} e^{-j\omega\tau} & \cdots & k_{2n} + j\omega c_{2n} \\ \vdots & \vdots & \ddots & \vdots & \ddots & \vdots \\ k_{r1} + j\omega c_{r1} & k_{r2} + j\omega c_{r2} & \cdots & k_{rr} - \omega^2 m_r + j\omega c_{rr} + \omega^2 g_{rr} e^{-j\omega\tau} & \cdots & k_{rn} + j\omega c_{rn} \\ \vdots & \vdots & \vdots & \vdots & \ddots & \vdots \\ k_{n1} + j\omega c_{n1} & k_{n2} + j\omega c_{n2} & \cdots & k_{nr} + j\omega c_{nr} + \omega^2 g_{nr} e^{-j\omega\tau} & \cdots & k_{nn} - \omega^2 m_n + j\omega c_{nn} \end{bmatrix}. \tag{20}$$

The acceleration FRF matrix $\mathbf{H}^D(\omega, \tau)$ of the delayed system can be written as

$$\mathbf{H}^D(\omega, \tau) = \frac{1}{\det(\mathbf{Z}^D(\omega, \tau))} \begin{bmatrix} A_{11}^D(\omega, \tau) & A_{21}^D(\omega, \tau) & \cdots & A_{r1}^D(\omega, \tau) & \cdots & A_{n1}^D(\omega, \tau) \\ A_{12}^D(\omega, \tau) & A_{22}^D(\omega, \tau) & \cdots & A_{r2}^D(\omega, \tau) & \cdots & A_{n2}^D(\omega, \tau) \\ \vdots & \vdots & \ddots & \vdots & \ddots & \vdots \\ A_{1r}^D(\omega) & A_{2r}^D(\omega) & \cdots & A_{rr}^D(\omega) & \cdots & A_{nr}^D(\omega) \\ \vdots & \vdots & \vdots & \vdots & \ddots & \vdots \\ A_{1n}^D(\omega, \tau) & A_{2n}^D(\omega) & \cdots & A_{rn}^D(\omega, \tau) & \cdots & A_{nn}^D(\omega, \tau) \end{bmatrix}, \tag{21}$$

where $\det(\mathbf{Z}^D(\omega, \tau))$ represents the determinant of $\mathbf{Z}^D(\omega, \tau)$, and $A_{pq}^D(\omega, \tau)$ is the algebraic cofactor of $\mathbf{Z}^D(\omega, \tau)$.

As can be seen in Eq. (21), all the algebraic cofactors of $\mathbf{Z}^D(\omega, \tau)$ are functions of ω . It should be noted that $A_{1r}^D(\omega), A_{2r}^D(\omega), \dots, A_{nr}^D(\omega)$ do not contain $e^{-j\omega\tau}$. This means elements in the r th row of $\mathbf{H}^D(\omega, \tau)$ do not contain $e^{-j\omega\tau}$ in their numerators. In other words, numerators of the elements in the r th row of $\mathbf{H}^D(\omega, \tau)$ are the same as those in the r th row of $\mathbf{H}(\omega)$. The expressions can be written as follows

$$\begin{aligned} H_{r\beta}^D &= \frac{A_{\beta r}^D}{\det(\mathbf{Z}^D(\omega, \tau))} \\ &= \frac{A_{\beta r}}{\det(\mathbf{Z}^D(\omega, \tau))}, \quad (\beta = 1, 2, \dots, n). \end{aligned} \tag{22}$$

According to Eqs. (13) and (18), we can obtain the relationship between $\det(\mathbf{Z}^D(\omega, \tau))$ and $\det(\mathbf{Z}(\omega))$:

$$\det(\mathbf{Z}^D(\omega, \tau)) = \det(\mathbf{Z}(\omega)) - \sum_{s=1}^n g_{sr} e^{-j\omega\tau} A_{sr}(\omega). \tag{23}$$

Since $\det(\mathbf{Z}(\omega))$ has been denoted by $\Phi(\omega)$, Eq. (23) can be rewritten as

$$\det(\mathbf{Z}^D(\omega, \tau)) = \Phi(\omega) - \sum_{s=1}^n g_{sr} e^{-j\omega\tau} A_{sr}(\omega). \tag{24}$$

Assume that point i is the input point. Then elements in the i th column of acceleration FRFs measured in the experiment can be expressed as

$$\{ H_{i1}^D(\omega, \tau) \ H_{i2}^D(\omega, \tau) \ \cdots \ H_{ir}^D(\omega, \tau) \ \cdots \ H_{in}^D(\omega, \tau) \}^T. \tag{25}$$

According to Eq. (21), the expression in Eq. (25) can be rewritten as

$$\frac{\{ A_{i1}^D(\omega, \tau) \ A_{i2}^D(\omega, \tau) \ \cdots \ A_{ir}^D(\omega) \ \cdots \ A_{in}^D(\omega, \tau) \}^T}{\det(\mathbf{Z}^D(\omega, \tau))}. \tag{26}$$

From Eq. (21) it can be seen that all FRFs have the same denominator, which inevitably contains a time delay τ . However, if the denominator and numerator of FRFs both contain τ , it is difficult to extract τ . To construct an algorithm to identify τ , an FRF whose numerator does not contain τ must be found.

According to Eqs. (22) and (26), $H_{ri}^D(\omega, \tau)$ can be measured in experiments. Moreover, it does not contain τ in its numerator. Therefore, $H_{ri}^D(\omega, \tau)$ is the right function to use to identify τ :

$$H_{ri}^D(\omega, \tau) = \frac{A_{ir}^D(\omega)}{\det(\mathbf{Z}^D(\omega, \tau))} = \frac{A_{ir}(\omega)}{\det(\mathbf{Z}^D(\omega, \tau))}. \tag{27}$$

Substituting Eq. (24) into Eq. (27), we obtain

$$H_{ri}^D(\omega, \tau) = \frac{A_{ir}(\omega)}{\Phi(\omega) - \sum_{s=1}^n g_{sr} e^{-j\omega\tau} A_{sr}(\omega)}. \tag{28}$$

In this paper, we define the pseudo-acceleration impedance functions at the reference point r of the uncontrolled and delayed system as

$$\begin{aligned} \tilde{Z}_{ri}(\omega) &= \frac{1}{H_{ri}(\omega)}, \\ \tilde{Z}_{ri}^D(\omega, \tau) &= \frac{1}{H_{ri}^D(\omega, \tau)}. \end{aligned} \tag{29}$$

Obviously, the pseudo-acceleration impedance function is the reciprocal of the FRF. It should be noted that the pseudo-acceleration impedance functions $\tilde{Z}_{ri}(\omega)$ and $\tilde{Z}_{ri}^D(\omega, \tau)$ are functions, while the acceleration impedance function matrices $\mathbf{Z}(\omega)$ and $\mathbf{Z}^D(\omega)$ are function matrices. Use “ \sim ” to show the difference between pseudo-acceleration impedance functions and acceleration impedance functions.

Substituting Eqs. (15) and (28) into Eq. (29), we obtain

$$\tilde{Z}_{ri}(\omega) = \frac{\Phi(\omega)}{A_{ir}(\omega)}, \tag{30}$$

$$\tilde{Z}_{ri}^D(\omega, \tau) = \frac{\Phi(\omega)}{A_{ir}(\omega)} - \frac{\sum_{s=1}^n g_{sr} e^{-j\omega\tau} A_{sr}(\omega)}{A_{ir}(\omega)}. \tag{31}$$

It can be seen that $\tilde{Z}_{ri}^D(\omega, \tau)$ consists of two parts. One is $\tilde{Z}_{ri}(\omega)$, the pseudo-acceleration impedance function at point i of the uncontrolled system. The other part is an amplitude-changing periodic function.

The difference between the two foregoing pseudo-acceleration impedance functions can be expressed as

$$\tilde{Z}_{ri}^D(\omega, \tau) - \tilde{Z}_{ri}(\omega) = -\frac{\sum_{s=1}^n g_{sr} A_{sr}(\omega)}{A_{ir}(\omega)} e^{-j\omega\tau}. \tag{32}$$

The amplitude of the difference function, namely, $\sum_{s=1}^n g_{sr} A_{sr}(\omega) / A_{ir}(\omega)$, is related to all the parameters except the time delay τ , while the “frequency” of the difference function is τ .

Therefore, the real part of the pseudo-acceleration impedance function of a delayed system can be treated as a superposition of the real part of the pseudo-acceleration impedance function of an uncontrolled system and a cosine curve, while the imaginary part of pseudo-acceleration impedance function of the delayed system can be treated as a superposition of the imaginary part of the pseudo-acceleration impedance function of the uncontrolled system and a sine curve. This means that if the difference between the real parts of the two pseudo-acceleration impedance functions is obtained, τ can be identified. Similarly, τ can also be identified from the difference between the imaginary parts of the two pseudo-acceleration impedance functions.

If the delayed system has only one feedback point f , Eq. (32) can be simplified to

$$\tilde{Z}_{ri}^D(\omega, \tau) - \tilde{Z}_{ri}(\omega) = -\frac{g_{fr} A_{fr}(\omega)}{A_{ir}(\omega)} e^{-j\omega\tau}. \tag{33}$$

3 Numerical simulation

In this section, numerical simulations in SDOF and MDOF systems are presented to apply the aforementioned identification approach.

3.1 Acceleration impedance function

For the SDOF delayed system described by Eq. (6), set $k = 500 \text{ N/m}$, $c = 1 \text{ N} \cdot \text{s/m}$, $m = 1 \text{ kg}$, $g = 0.5 \text{ N} \cdot \text{s}^2/\text{m}$, and $\tau = 0.2 \text{ s}$. Since there is only one point, the input point, reference point, and feedback point merge into one.

The curves of the uncontrolled system and delayed system are shown in Fig. 1a shows the curves of the acceleration FRFs, while Fig. 1b shows the curves of the acceleration impedance functions.

The difference functions of the two acceleration impedance functions in Fig. 1b, with the real part and imaginary part separated, are shown in Fig. 2.

After performing fast Fourier transform (FFT) on the data in Fig. 2, we get the “frequencies” of the difference curves. It can be seen from Fig. 3 that the “frequency” of the difference curve of the two real parts is 0.1992 s, which is very close to the value of the time delay τ set at the beginning of the simulation (0.2 s). τ can also be identified from the difference curve of the two imaginary parts.

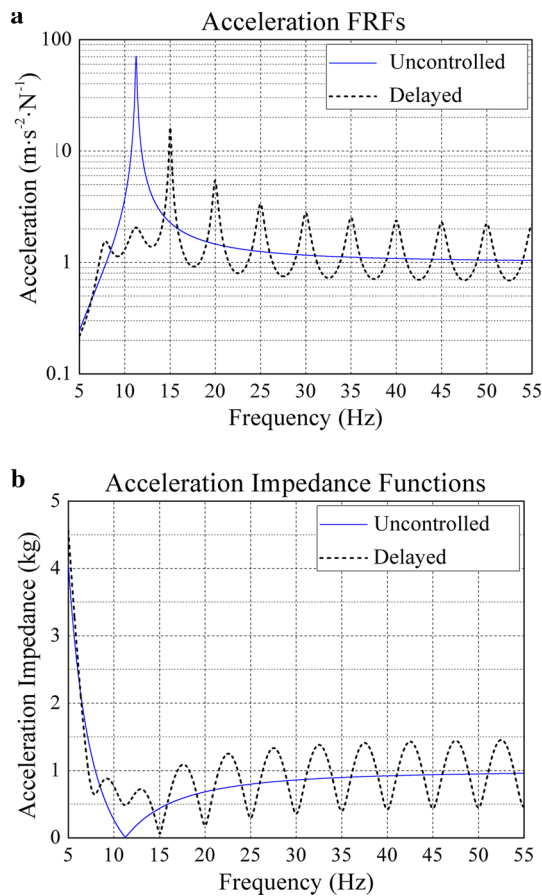


Fig. 1 Curves of uncontrolled system and delayed system. **a** Curves of acceleration FRFs. **b** Curves of acceleration impedance functions

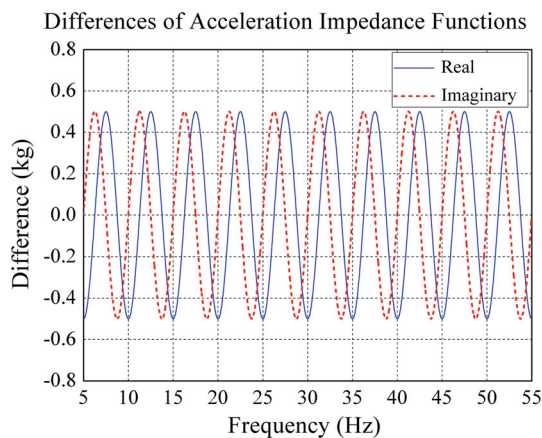


Fig. 2 Difference curves of acceleration impedance functions

3.2 Pseudo-acceleration impedance function

To apply the aforementioned identification approach, a 5-DOF system was constructed (Fig. 4).

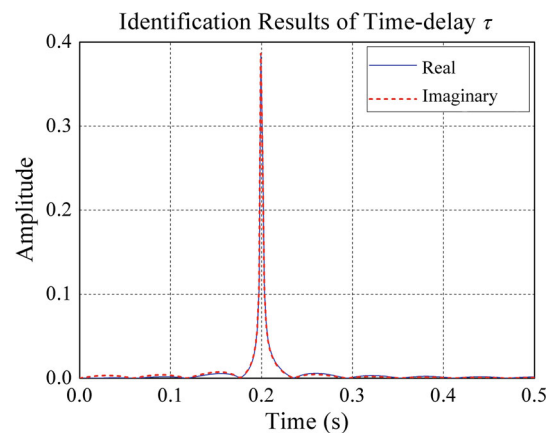


Fig. 3 Identification results of time delay ($\tau = 0.2$ s)

Assume that $m_1 = 4$ kg, $m_2 = 3$ kg, $m_3 = 1$ kg, $m_4 = 4$ kg, $m_5 = 3$ kg, $k_2 = k_3 = 20,000$ N/m, $k_2 = k_3 = 20,000$ N/m, and $k_0 = k_1 = k_4 = k_5 = 40,000$ N/m. The damping ratios of each order are $\{2 \ 2 \ 2 \ 2 \ 1\} \times 10^{-3}$. The feedback gain is $0.5 \text{ N} \cdot \text{s}^2/\text{m}$. The time delay τ is 0.5 s.

3.2.1 Single feedback

First, the delayed system with a single feedback is examined in what follows. Set m_3 as the reference point and m_4 as the feedback point (Fig. 5).

The acceleration FRFs at the reference point m_3 can be obtained, namely, $H_{35}(\omega)$ and $H_{35}^D(\omega, \tau)$, as shown in Fig. 6a. $H_{35}(\omega)$ is the acceleration FRF of the uncontrolled system, while $H_{35}^D(\omega, \tau)$ is the acceleration FRF of the delayed system. Accordingly, the two pseudo-acceleration impedance function curves at the reference point m_3 can also be obtained, namely, $PAI_{35}(\omega)$ and $PAI_{35}^D(\omega, \tau)$, as shown in Fig. 6b.

The difference functions of the two acceleration impedance functions in Fig. 6b, with the real and imaginary parts separated, are shown in Fig. 7.

By performing an FFT on the data in Fig. 7, we obtain the “frequencies” of the difference curves. As shown in Fig. 8, the “frequency” of the difference curve of the two real parts is 0.5 s, which is exactly the value of the time delay τ set at the beginning of the simulation. τ can also be identified from the difference curve of the two imaginary parts.

3.2.2 Multiple feedback

Now we consider a delayed system with multiple feedback. Assume that the feedback gains are $0.5 \text{ N} \cdot \text{s}^2/\text{m}$. The time delay τ is 0.5 s. Set m_3 as the reference point and all the measuring points as the feedback points (Fig. 9).

The acceleration FRFs at the reference point m_3 can be obtained, namely, $H_{35}(\omega)$ and $H_{35}^D(\omega, \tau)$, as shown in

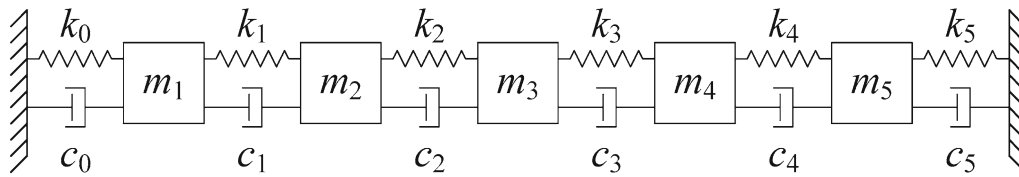


Fig. 4 A 5-DOF mechanical model

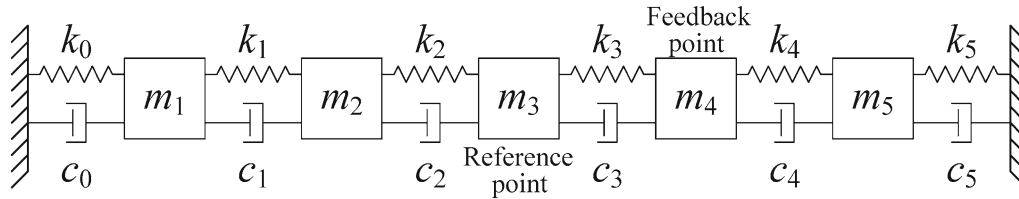


Fig. 5 A 5-DOF mechanical model with single feedback point

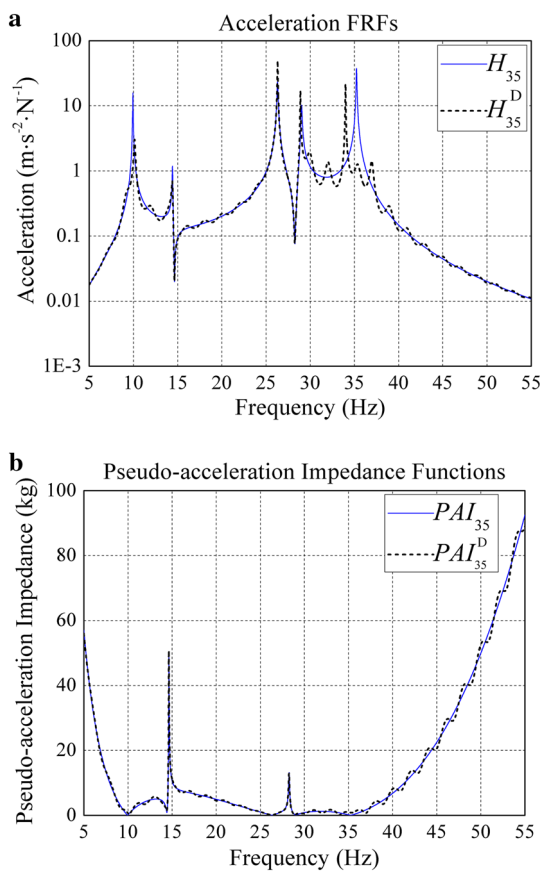


Fig. 6 Curves of uncontrolled system and delayed system. **a** Curves of acceleration FRFs. **b** Curves of pseudo-acceleration impedance functions

Fig. 10a. $H_{35}(\omega)$ is the acceleration FRF of the uncontrolled system, while $H_{35}^D(\omega, \tau)$ is the acceleration FRF of the delayed system. Accordingly, the two pseudo-acceleration impedance function curves at the reference point m_3 can also be obtained, namely, $PAI_{35}(\omega)$ and $PAI_{35}^D(\omega, \tau)$, as shown in Fig. 10b.

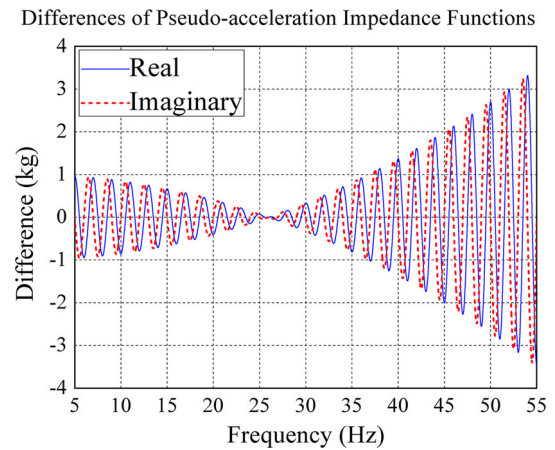


Fig. 7 Difference curves of pseudo-acceleration impedance functions

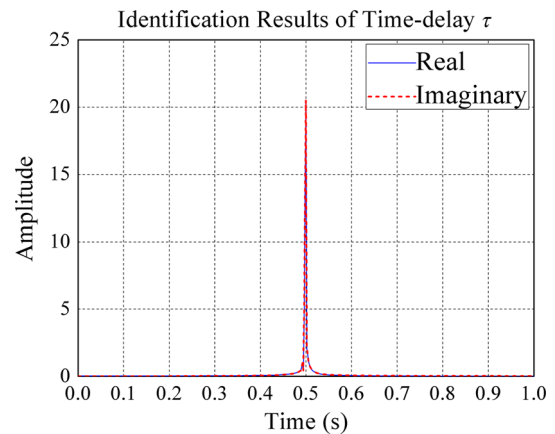


Fig. 8 Identification results of time delay ($\tau = 0.5$ s)

The differences between the real and imaginary parts of the two pseudo-acceleration impedance functions in Fig. 10b can be separated, as shown in Fig. 11.

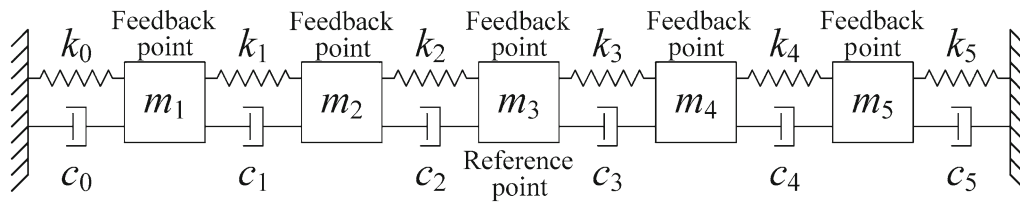


Fig. 9 5-DOF mechanical model with multiple feedback points

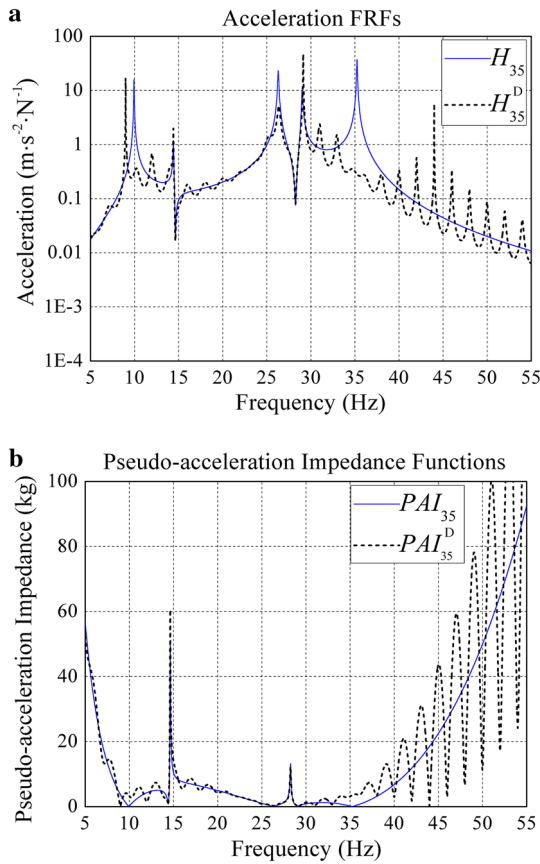


Fig. 10 Curves of uncontrolled and delayed systems. **a** Curves of acceleration FRFs. **b** Curves of pseudo-acceleration impedance functions

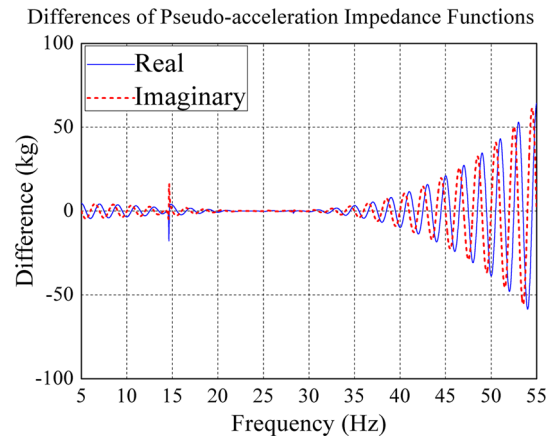


Fig. 11 Difference curves of pseudo-acceleration impedance functions

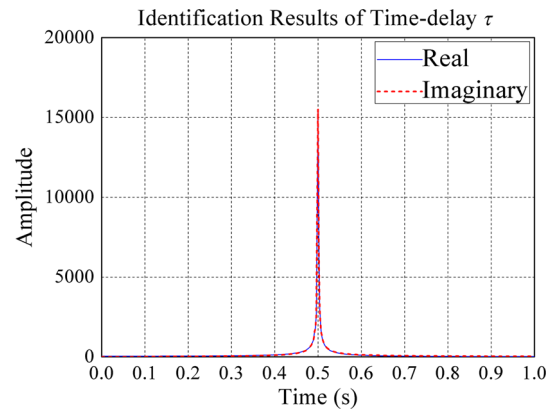


Fig. 12 Identification results of time delay ($\tau = 0.5$ s)

By performing an FFT on the data in Fig. 11, we obtain the “frequencies” of the difference curves. As shown in Fig. 12, the “frequency” of the difference curve of the two real parts is 0.5 s, which is exactly the value of the time delay τ set at the beginning of the simulation. τ can also be identified from the difference curve of the two imaginary parts.

According to the preceding numerical simulations, the difference functions between the curves of the uncontrolled system and delayed system are periodic functions in the frequency domain. The fact that the time delay τ is the “frequency” of the periodic functions is the principle of the proposed identification approach.

4 Experiment

To verify the aforementioned identification approach, an experiment is conducted (Fig. 13).

The aluminum block, the actuator, and the four connecting aluminum blocks on the top of the four rubber isolators are all fixed. They constitute vibration-isolated substances. The size of the slab foundation is 700 mm × 500 mm × 2 mm. The two long sides are clamped, while the other sides are free. To approach the condition of clamping, six $\Phi 8$ high-strength bolts are used on the long sides. To avoid the effects of collision between the slab foundation and steel angles for

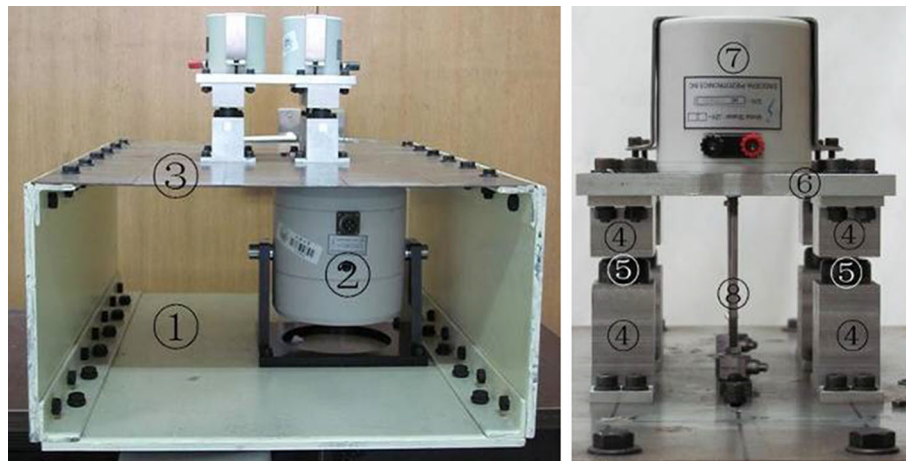


Fig. 13 Experimental devices. The photo on the left shows a panoramic view of the test unit, while the one on the right shows the upper part of the test unit. The test unit consists of the following parts: ① cabinet base, ② input source, ③ slab foundation, ④ link block, ⑤ rubber isolator, ⑥ aluminum block, ⑦ actuator, ⑧ connecting rod and force sensor

clamping, a damping layer is placed between them. The cabinet base consists of a 10 mm steel plate on the left side, right side, and bottom. Between the two sides, steel angle and high-strength bolts are applied to prevent obvious vibration modes in the frequency band (0–200 Hz) concerned.

4.1 Time-delay feedback experiment

With respect to the time delay feedback experiment, the arrangement of the measuring points is shown in Fig. 14. The input point is point 37. The reference point is point 41. The feedback point is also point 41. Several groups of experiments are conducted with different time delay values applied to the system.

As an example, we consider a delayed system with a time delay τ of 1.0 s to explain the process of identification. The identification results of the other time delay values are shown in the last part of Sect. 4.2.

Figure 15 shows the acceleration FRF and pseudo-acceleration impedance function at the reference point.

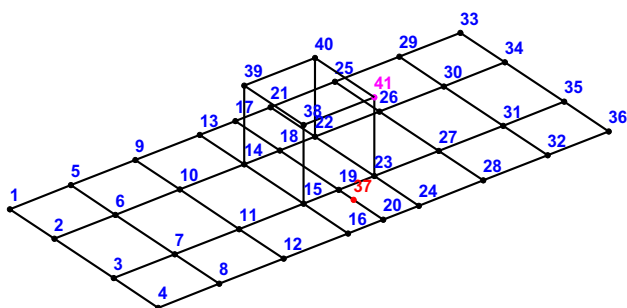


Fig. 14 Distribution of measuring points

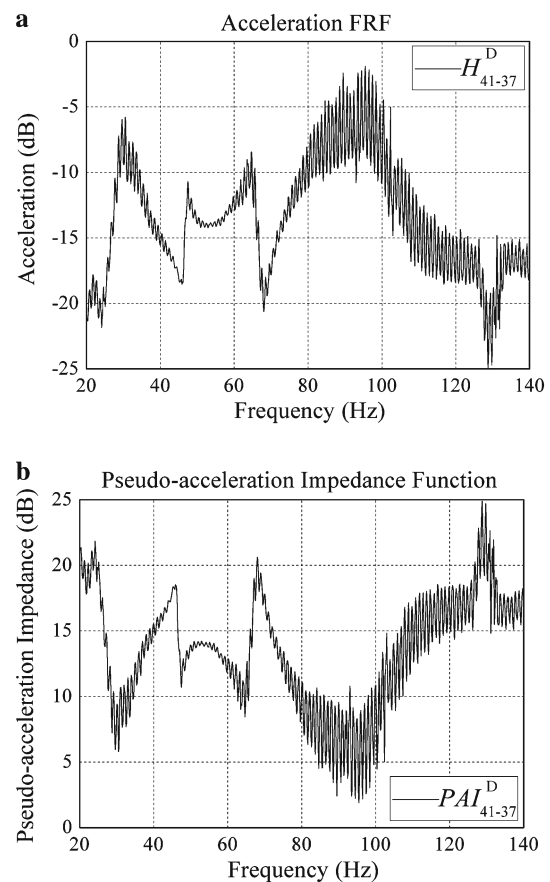


Fig. 15 Curves of delayed system with $\tau = 1.0$ s. **a** Curve of acceleration FRF H_{41-37}^D . **b** Curve of pseudo-acceleration impedance function PAI_{41-37}^D

As explained in the aforementioned identification approach, the oscillation of the acceleration FRFs is caused by the time delay τ . This means τ can be identified from

the difference between the real parts (or the imaginary parts) of the two pseudo-acceleration impedance functions of the uncontrolled and delayed systems.

However, in the time delay feedback experiment, what we obtain are the FRF curves of the delayed system, which means the curves of the uncontrolled system are not available. Thus, the curves of the uncontrolled system, namely, the trend lines, should first be removed by a numerical method. In this paper, the empirical mode decomposition (EMD) method [22] is employed to remove the trend lines.

4.2 Identification results

The results of the EMD method can be divided into at least two parts. One part is the trend line that contains the modal information of the uncontrolled system. The other part is an oscillation curve with a zero centerline. This curve includes information on the time delay τ .

Figure 16 displays the results of EMD for the original curve shown in Fig. 15b. The first component, namely, the trend line, is shown in Fig. 16a, while the oscillation curve containing the time delay τ is shown in Fig. 16b. After the

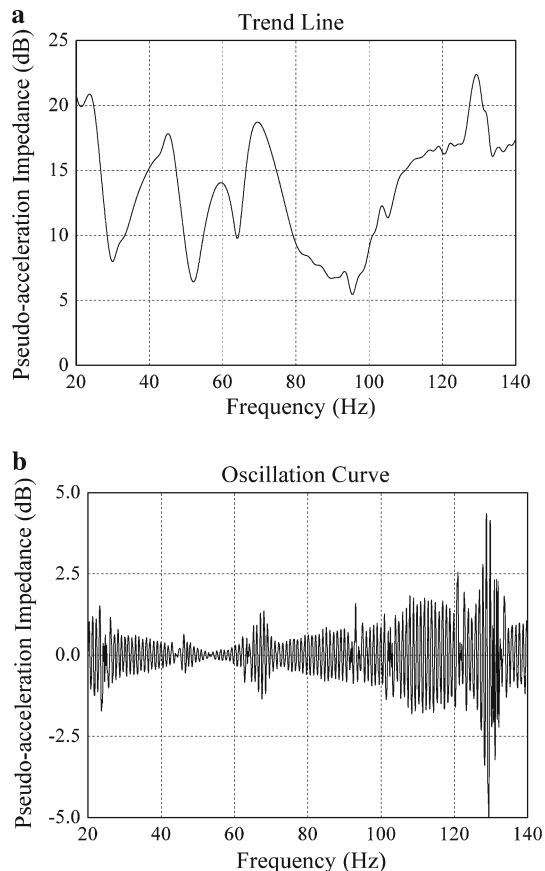


Fig. 16 Results of EMD for pseudo-acceleration impedance function of delayed system. **a** Trend line. **b** Oscillation curve containing τ

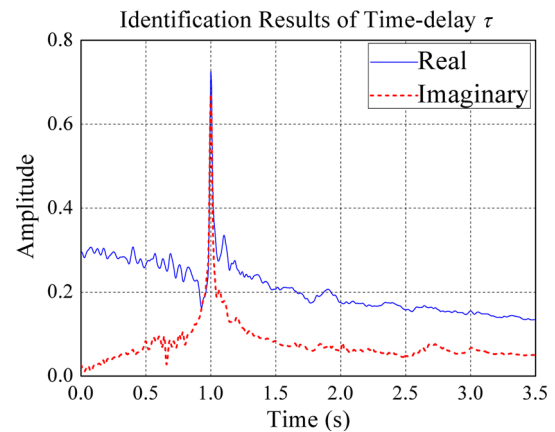


Fig. 17 Identification results of delayed system ($\tau = 1.0$ s)

Table 1 Identification results of time delay

Set value (s)	Identified value (s)	Absolute error (s)	Relative error (%)
0.2000	0.1999	-0.0001	0.05
0.2500	0.2479	-0.0021	0.84
0.3000	0.2998	-0.0002	0.07
0.4000	0.4007	0.0007	0.18
0.5000	0.5007	0.0007	0.14
0.6000	0.5997	-0.0003	0.05
0.7000	0.7005	0.0005	0.07
0.8000	0.7996	-0.0004	0.05
0.9000	0.9022	0.0022	0.24
1.0000	1.0007	0.0007	0.07

real and imaginary parts of the original curve are separated, the curves of these two parts can be decomposed using the EMD method.

By performing an FFT on the oscillation curve in Fig. 16b with the real and imaginary parts separated, the “frequencies” of the curves can be obtained. It can be seen from Fig. 17 that the “frequency” of the real part is 1.002 s, which is very close to the value of the time delay τ set at the beginning of the time delay feedback experiment. The time delay τ identified from the imaginary part is 1.0 s, which is the same as the value at which τ was set.

Several groups of experiments are conducted with different time delay values applied to the system. The process of identification is the same as earlier. The identification results are shown in Table 1.

It can be seen from Table 1 that the identification results have a high accuracy. Specifically, the maximum absolute error is 0.0022 s in the case where the time delay is 0.9 s. The maximum relative error is 0.84% in the case where the time delay is 0.25 s.

5 Conclusions

This paper presented an time delays in linear systems. First, in SDOF systems, the relationships between time delays and impedance functions of uncontrolled and delayed systems were derived. The time delay is the “frequency” of the difference curve of the two impedance functions. This is the principle of the identification approach.

Second, in MDOF systems, the impedance function matrix is the inverse matrix of the FRF matrix. Because FRF matrixes cannot be completely measured in experiments, a pseudo-impedance function, the reciprocal of the FRF, was defined. Then the relationships between the time delay and pseudo-impedance functions of uncontrolled and delayed systems were deduced. The time delay was identified from the difference curve of the two pseudo-impedance functions.

Apart from numerical simulations of an SDOF system and a 5-DOF system, an experiment was conducted on an MDOF delayed system with acceleration feedback to verify the identification approach. Although the FRF curve of the delayed system was measured in experiments, that of the corresponding uncontrolled system was not available. This means the curve of the pseudo-impedance function of the uncontrolled system could not be obtained. Then the EMD method was used to remove the trend line of the curve of the pseudo-impedance function of the delayed system. The trend line was actually the curve of the pseudo-impedance function of the uncontrolled system. The time delay was identified from the remaining oscillation curve. Different time delay values were applied to the MDOF system. The identification results of the time delay using the proposed identification approach showed the faithfulness of the approach.

Acknowledgements This project was supported by the National Natural Science Foundation of China (Grant 11272235).

References

- Hong, T., Hughes, P.C.: Effect of time delay on the stability of flexible structures with rate feedback control. *J. Vib. Control* **7**, 33–49 (2001)
- Xu, J., Chung, K.W.: Effects of time delayed position feedback on a van der Pol–Duffing oscillator. *Physica D—Nonlinear Phenomena* **180**, 17–39 (2003)
- Hu, H.Y.: Using delayed state feedback to stabilize periodic motions of an oscillator. *J. Sound Vib.* **275**, 1009–1025 (2004)
- Qin, Y.X., Liu, Y.O., Wang, L., et al.: *The Motion Stability of Dynamical Systems with Time-Delay*, 2nd edn. Science Press, Beijing (1989). (in Chinese)
- Mohamed, A.R.: Time-delay effects on actively damped structures. *J. Eng. Mech.* **113**, 1709–1719 (1987)
- Chu, S.Y., Soong, T.T., Lin, C.C., et al.: Time-delay effect and compensation on direct output feedback controlled mass damper systems. *Earthq. Eng. Struct. Dyn.* **31**, 121–137 (2002)
- Olgac, N., Holmhansen, B.T.: A novel active vibration absorption technique-delayed resonator. *J. Sound Vib.* **176**, 93–104 (1994)
- Udwadia, F.E., von Bremen, H., Phohomsiri, P.: Time-delayed control design for active control of structures: principles and applications. *Struct. Control Health Monit.* **14**, 27–61 (2007)
- Campbell, S.A., Crawford, S., Morris, K.: Friction and the inverted pendulum stabilization problem. *J. Dyn. Syst. Meas. Control* **130**, 556–562 (2008)
- Cai, G.P., Lim, C.W.: Optimal tracking control of a flexible hub-beam system with time delay. *Multibody Syst. Dyn.* **16**, 331–350 (2006)
- Xu, J., Sun, Y.X.: Experimental studies on active control of a dynamic system via a time-delayed absorber. *Acta Mech. Sin.* **31**, 229–247 (2015)
- Wang, Z.H., Hu, H.Y.: A modified averaging scheme with application to the secondary Hopf bifurcation of a delayed van der Pol oscillator. *Acta Mech. Sin.* **24**, 449–454 (2008)
- Palkovics, L., Venhovens, P.J.Th.: Investigation on stability and possible chaotic motions in the controlled wheel suspension system. *Veh. Syst. Dyn.* **21**, 269–296 (1992)
- Fofana, M.S.: Effect of regenerative process on the sample stability of a multiple delay differential equation. *Chaos Solitons Fractals* **14**, 301–309 (2002)
- Orlov, Y., Belkoura, L., Richard, J.P., et al.: On-line parameter identification of linear time-delay systems. In: *IEEE Conference on Decision & Control*, Las Vegas, Nevada, USA, 630–635 (2002)
- Hidayat, E., Medvedev, A.: Laguerre domain identification of continuous linear time-delay systems from impulse response data. *Automatica* **48**, 2902–2907 (2012)
- Gu, W.D., Sun, Z.Y., Wu, X.M., et al.: Simultaneous identification of unknown time delays and model parameters in uncertain dynamical systems with linear or nonlinear parameterization by autosynchronization. *Chin. Phys. B* **22**, 190–196 (2013)
- Na, J., Ren, X.M., Xia, Y.Q.: Adaptive parameter identification of linear SISO systems with unknown time-delay. *Syst. Control Lett.* **66**, 43–50 (2014)
- Karoui, A., Ibn Taarit, K., Ksouri, M.: Algebraic identification approach of multiple unknown time-delays of continuous-time linear systems. *Adv. Intell. Syst. Comput.* **427**, 315–325 (2016)
- Hu, H.Y.: Identifiability of feedback delays of linear controlled systems. *J. Vib. Eng.* **14**, 161–165 (2001). (in Chinese)
- Brincker, R., Ventura, C.E.: *Introduction to Operational Modal Analysis*. Wiley, West Sussex (2015)
- Huang, N.E., Shen, Z., Long, S.R., et al.: The empirical mode decomposition and the Hilbert spectrum for nonlinear and non-stationary time series analysis. *Proc. R. Soc. A Math. Phys. Eng. Sci.* **454**, 903–995 (1998)